Dear Reviewer, #2

Thank you very much for your valuable comments. Our responses and the changes that we plan to make in the revised manuscript are explained below. We filled in reviewer comments in black, author replies in blue, the proposed changes to the revised manuscript in red.

Reviewer comment:

First, data from the ST9 snow pit indicate evidence of summer surface snowmelt. Such melting processes hinder the preservation of proxy records and introduce uncertainty in age-dating. As discussed in the manuscript (lines 164–165), water isotope records tend to become smoothed, and ion concentrations are altered due to refreezing of meltwater. Therefore, the interpretation of vertical variations in proxy concentrations should account for these site-specific characteristics. Particularly in Section 3.2 ("Spatial and temporal variations in water isotopes and chemical species"), the interpretation of ST9 data should reflect the impact of summer melt on concentration variability.

Author reply:

As you have pointed out, the water stable isotopes were smoothed and ion concentrations were relocated due to meltwater refreezing. Therefore, the amplitude of the seasonal variations in water stable isotopes were smaller and ion concentrations showed high peaks in the ice layer. We have already described the impact of the melt water refreezing on the seasonality of water stable isotopes and ion concentrations in our manuscript as follows.

=====

3.1 Snowpack dating and annual accumulation

~~~ The MSA concentration showed obvious seasonal variations, and the $\delta^{18}O$ values exhibited slight seasonal variations below 0.96 m (Fig. 2a and c), although the values of the water stable isotopes were smoothed by summer melting and some chemical species showed high peaks in the ice layers owing to relocation processes by meltwater refrozen. ~~~

3.2 Spatial and temporal variations in $\delta^{18}O$ and chemical species

~~~ The concentrations of NO_3^- at St. 9 showed several peaks at depths of 0.01, 1.07, 1.94, 2.37, 2.87, 3.15, and 3.57 m (Fig. 7). According to the stratigraphy of the snowpack at St. 9, we attributed the peaks at 0.01, 1.07, 1.94 and 3.15 m to the deposition of atmospheric nitrate and the peaks at 2.37, 2.87 and 3.57 m to melting and refreezing process. ~~~

=====

Reviewer comment:

The seasonal classification such as spring–summer vs. autumn–winter should be used consistently, and the discussion of concentration variability should be supported by statistical criteria due to no clear variability of proxies. For example, it is recommended to define peaks using either values above the mean or above the mean plus one standard deviation.

Author reply:

In accordance with your comment, we will unify the description of seasonal classification as spring-summer and autumn-winter.

We will define positive (negative) peaks of each ion according to statistical criteria, which were values above (below) the mean plus (minus) one standard deviation.

Reviewer comment:

Second, additional evidence is required to substantiate some of the manuscript's interpretations. For example, to support the discussion on atmospheric transport, the inclusion of backward trajectory modeling (e.g., frequency maps and cluster analyses) is recommended as supplementary information to identify source regions and air mass pathways.

Author reply:

Thank you for your valuable suggestion.

This study suggested that the oceanic aerosols were transported from the area near the western side of Prudhoe Land, located on the NOW, throughout the year by analyzing $\delta^{18}O$ and chemical species in the snowpack in western side of Prudhoe Land. To make this assumption more reliable, we performed the backward trajectory analysis and created a frequency map of the air mass transportation (Fig. 1 in this file). Majority of air mass arriving at western side of Prudhoe Land was transported from southern Greenland via northern Baffin Bay and eastern NOW. The existing probability in the eastern NOW was particularly high. The backward trajectory analysis supported our assumption, which the primary source of oceanic aerosols was NOW polynya throughout the year.

Figure 1 in this file will be added to the supplementary material, and relevant explanations will also be added in our revised manuscript.

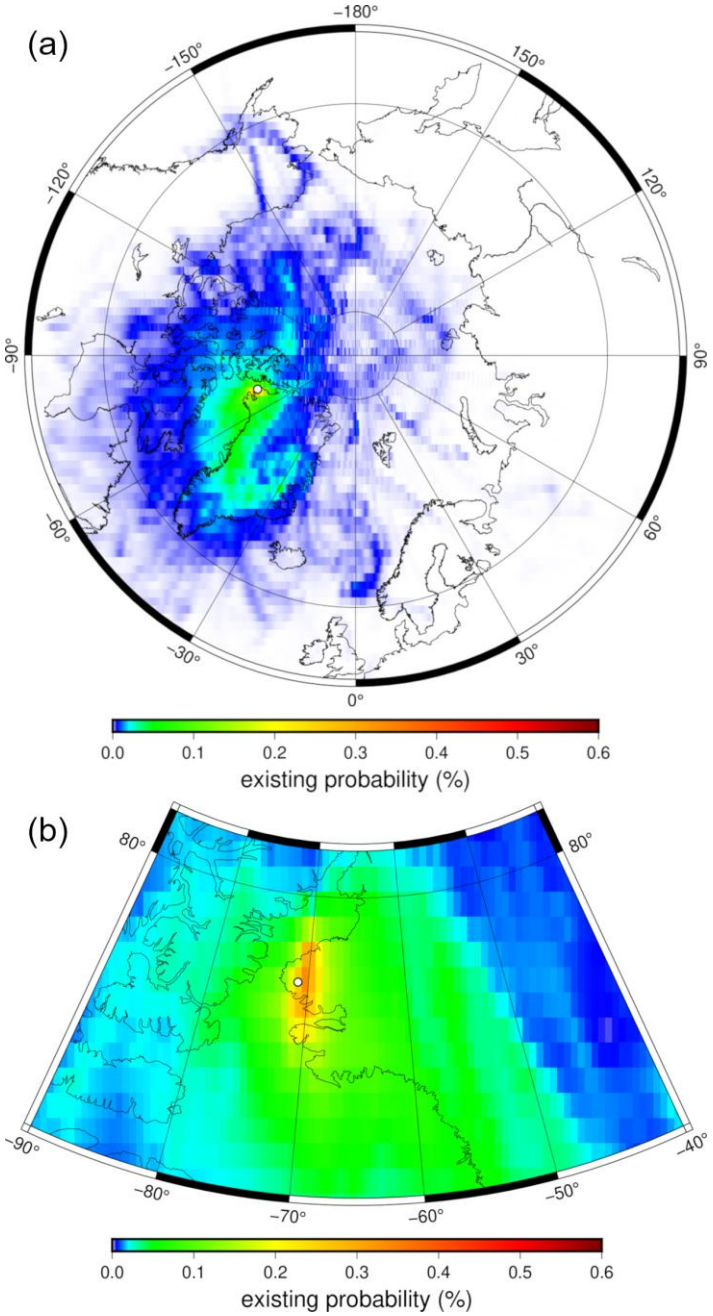

Figure 1 (in this file): Existence probability of an air mass occurring during the past during 7 days reaching the St. 9 in whole of year from 2019–2023. (a) and (b) display Arctic area (> 60°N) and around northwestern Greenland, respectively. Black circles show the position of the St. 9.

Reviewer comment:

Lines 44–70: The necessity of studying past environmental changes in the NOW region is well presented. However, further explanation is needed on how the current study site differs from the nearby SIGMA-A site, especially in terms of meteorological conditions like prevailing wind directions.

Author reply:

We will add a description of how this study site differs from the nearby SIGMA-A site, as follows.

=====

In the Prudhoe Land, a gentle valley separates the western region from the eastern region, where the SIGMA-A site is situated. (Fig. 1b). This valley could serve as a pathway for air masses transported from inland of the Greenland Ice Sheet to descend toward the coastal region, and these air masses are likely not transported to the western side of Prudhoe Land. If that is the care, the snowpack on the western part of Prudhoe Land could contain aerosols originating from the NOW without being mixed with aerosols from the interior of the Greenland Ice Sheet.

=====

Reviewer comment:

Line 68–69: Rephrase for clarity.

Author reply:

We have revised the text you kindly pointed out as follows.

=====

Water vapor and sea salt on the glacier facing the ocean were transported from the coast. On the other hand, water vapor, mineral dust, anthropogenic substances, and MSA on the eastern side of Prudhoe Land were transported from the central-west coast of Greenland, which is located around Disko Bay, via the central part of the Greenland Ice Sheet (Matoba et al., 2014).

=====

Reviewer comment:

Lines 104–105: Add information in the Supplementary Information regarding the design and cleaning procedures of the pre-cleaned stainless-steel tools used for snow pit sampling. Clarify the cleanliness specification of the Whirl-Pak polyethylene bags (e.g., part number, manufacturer).

Author reply:

We removed the oil contamination on the precleaned materials and tools using ethanol, and performed then ultrasonic cleaning in ultrapure water. The ®Whirl-Pak polyethylene bags were produced by Nasco. We will add this description to our revised manuscript.

Reviewer comment:

Because sample depth resolution varies (2 cm, 3 cm, 5–10 cm), figures such as Figure 4 should adopt a step-wise format for clarity, not dot and line format.

Author reply:

In accordance with your comment, we have changed figure plots of water stable isotopes and ion concentrations to step-wise format (ex. Fig. 2 in this file).

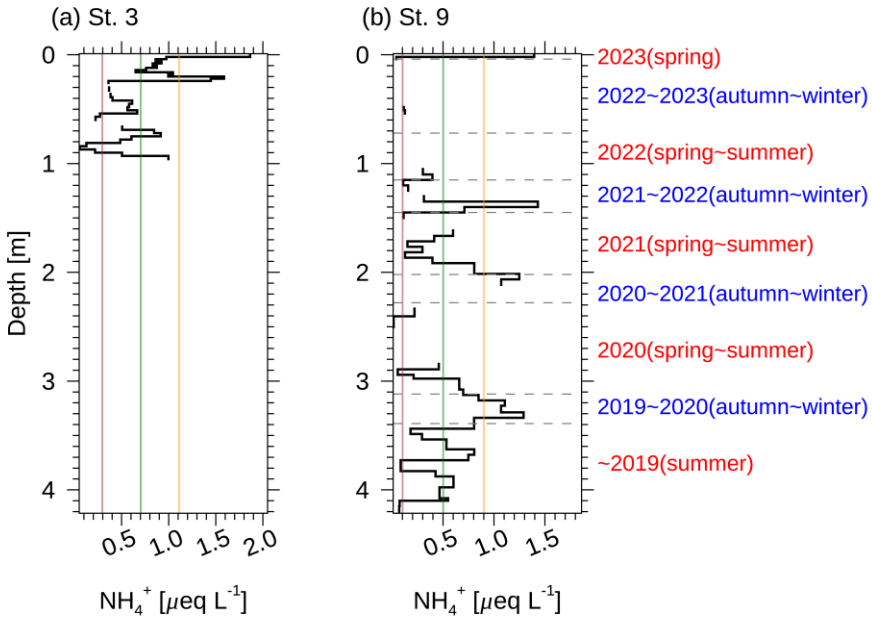

Figure 2 (in this file): Vertical profile of NH_4^+ at (a) St. 3 and (b) St. 9. Green lines denote mean NH_4^+ across all observation depths. Orange and brown lines denote the mean NH_4^+ plus and minus one standard deviation across all observation depths, respectively. The LOD of NH_4^+ was < 0.0055 μeq L^{-1}.

Reviewer comment:

Line 112: Provide details about possible contamination during snow sample melting and bottling. if possible, field blank should be provided.

Author reply:

We did not make a field brank in this observation. The field brank from our previous research (Kurosaki et al., 2020), which was made following the same procedure as used in this observation, was below the detection limit in the ion chromatography analysis.

Reviewer comment:

Line 117: Include specifications of the analytical column (e.g., length, diameter), model/manufacturer of standard materials, and detection limits for each ion.

Author reply:

As you have commented out, we will include the details of analytical column, standard materials, and detections limits as follows.

=====

For the cations, separation was carried out with a Dionex CG-12 (4 × 50 mm) guard column, followed by a Dionex CS12-A (4 × 250 mm) separation column. Injection volume of samples was 500 μL. MSA (20 mM) was used as eluent, and flow-rate was kept 1.0 mL min-1. Dionex CDRS600 dynamically regenerated suppressor was used for

conductivity suppression before conductivity cell. For the anions, separation was obtained with a Dionex AG-18 (4 × 50 mm) guard column and Dionex AS-18 (4 × 250 mm) separation column. Injection volume of samples was 1000 µL. KOH (23 mM) was used as eluent, and flow-rate was kept 1.0 mL min^{-1}. Dionex ADRS 600 dynamically regenerated suppressor was used for conductivity suppression before conductivity cell. 5-point calibration curves were used for quantitative determination of each ion. The 5-point calibration curves were constructed using standard solution (Fujifilm Waco) adjusted to 20, 50, 100, and 200 ppb with ultra-pure water. If the ion concentration of samples were outside the calibration range (> 200 ppb), it was remeasured using 500, 1000, 2000~3000, and 6000 ppb standard for the anions and 500, 1000, 2000, and 4000 ppb standard for the cations. Blanks were always evaluated before the calibration procedure. The analytical precision of the ion chromatography was < 5 % (at the measurement of 20 ppb standard). The limit of detection (LOD) was < 0.1 ppb. The limit of quantification (LOQ) was < 0.5 ppb.

=====

Reviewer comment:

Line 122: Specify the standard material used for stable water isotope analysis.

Author reply:

We will add the standard materials used for stable water isotope analysis in the method section as follows.

=====

We used the ultrapure water ($\delta^{18}O = -11.583$ and $\delta D = -77.2$), Antarctic iceberg ($\delta^{18}O = -20.4$ and $\delta D = -158.7$), snowpack on the Antarctic ice Sheet ($\delta^{18}O = -46.694$ and $\delta D = -370.7$) for calibration.

=====

Reviewer comment:

Line 139: Present snow density alongside depth.

Author reply:

We will add the vertical snow density in our supplementary materials (Fig. 3 in this file).

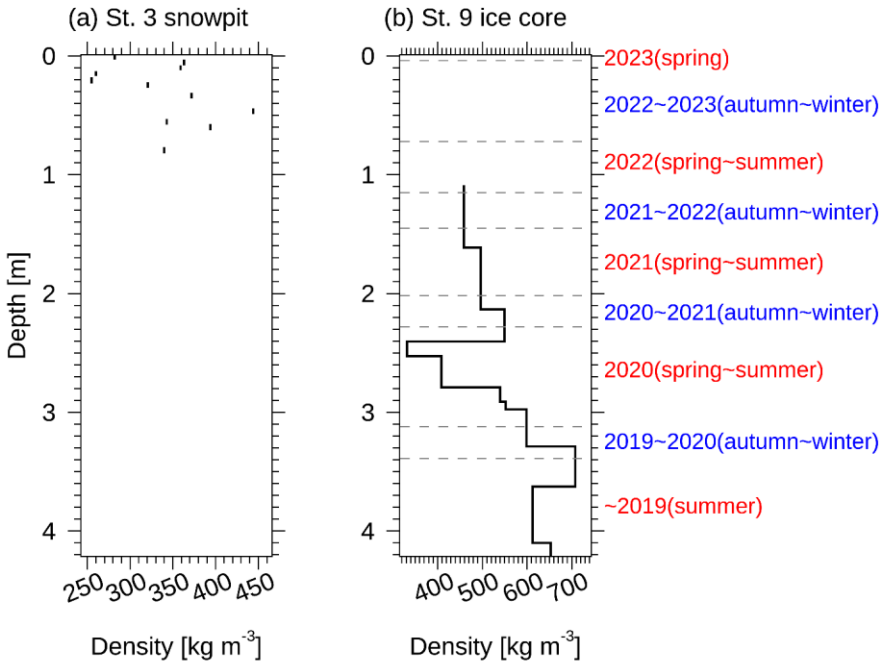

Figure 3 (in this file): Vertical profiles of the snow density at (a) St.3 and (b) St.9.

Reviewer comment:

Lines 143–144: Ice layers below 0.96 m in the ST9 snowpack suggest summer melting, which may affect proxy preservation. This is appropriately and kindly described in lines 163–168.

Author reply:

As you have pointed out, we also think that the ion concentrations showed high values in the ice layers due to meltwater refreezing. Therefore, we attributed the peaks at the ice layers to meltwater refreezing and the other peaks to the deposition of atmospheric aerosols. We have already described this sentence in our manuscript.

Reviewer comment:

Line 172: Calculate annual accumulation rates using snow density for each depth interval and present average values.

Author reply:

As you have pointed out, we calculated annual accumulation rates using snow density for each depth interval. We will revise the text regarding the annual accumulation rates as follows.

=====

According to the snowpack dating approach described above, the snow densities, which were the average of the bulk density of ice core at St. 9 (Fig. S3), from autumn–winter 2020 to autumn–winter 2021 and from autumn–winter 2019 to autumn–winter 2020 were 477 kg m^{-3} and 497 kg m^{-3}, respectively. Using these mean densities, the annual accumulations were calculated to be 0.41 m w.eq. yr^{-1} and 0.56 m w.eq. yr^{-1}, respectively.

=====

Reviewer comment:

Line 183: Indicate the MSA detection limit as a line in Figure 4. Clarify dating below 3.4 m at ST9 (the conclusion mentions dating down to 4.5 m).

Author reply:

We have included the limit of detections (LOD) for each ion in captions of related figures because they were too small to be clearly shown in the figures.

We will edit the captions as follows:

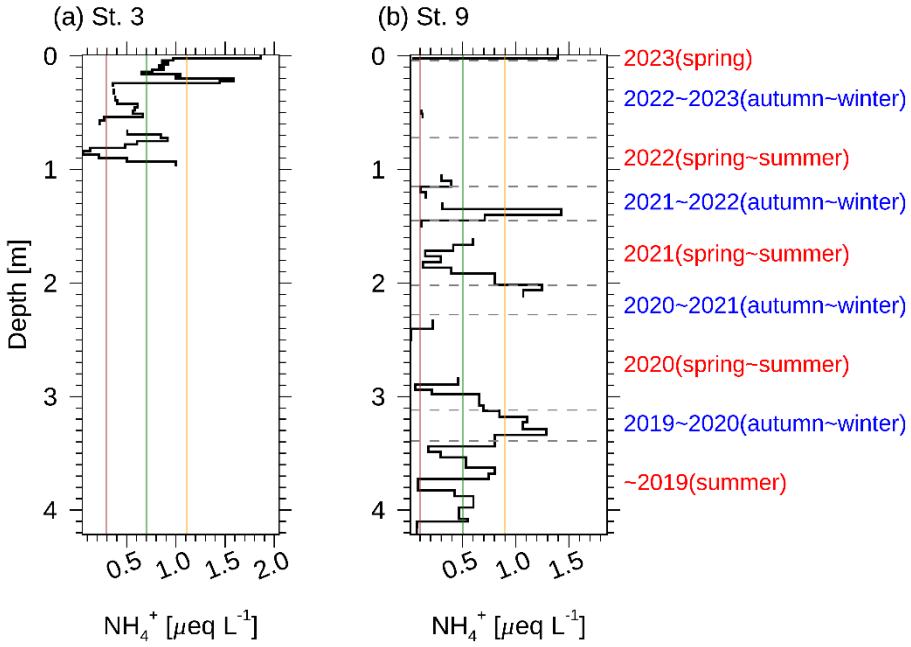

Figure 5 (in this file): Vertical profile of NH_4^+ at (a) St. 3 and (b) St. 9. Green lines denote mean NH_4^+ across all observation depths. Orange and brown lines denote the mean NH_4^+ plus and minus one standard deviation across all observation depths, respectively. The LOD of NH_4^+ was < 0.0055 μeq L^{-1}.

Reviewer comment:

Line 188: Include NO3- data.

Author reply:

We have deleted the relevant sentence, following the suggestion of another reviewer.

Reviewer comment:

Line 196: Use nss-Ca2+ to interpret dust transport. Since nss-K+ and nss-Mg2+ mostly show negative values, suggesting major marine influence, omit these from discussion and Table 1.

Author reply:

As you have commented out, we have removed the nss-Mg2+ and nss-K+ in our discussion and Table 1.

Reviewer comment:

Lines 197–209: Explain shortly the notable difference in $\delta^{18}O$ between the upper layer (0–0.7 m) and the deeper layer.

Author reply:

The snow stratigraphy from 0.0 to 0.96 m at St. 9 were the rounded grains, faceted crystals, or depth hoar, whereas the melt forms prevailed below 0.96 m. The $\delta^{18}O$ in the snowpack below 0.96 m were smoothed by melting, thereby seasonal variations in $\delta^{18}O$ were smaller than the upper layer.

We have already described this sentence in our manuscript as follows.

=====

Snowpack below 0.96 m corresponded to previous summer and before it because the amplitude of seasonal variation of $\delta^{18}O$ and d-excess below 0.96 m were smaller than those in the shallower layers from 0.00–0.96 m because of summer melting.

=====

Reviewer comment:

Line 201: Present backward trajectory modeling results to support atmospheric transport path interpretations.

Author reply:

In accordance with your comment, we will add backward trajectory analysis (Fig. 1 in this file). We suggested that the south-to-north gradient of the $\delta^{18}O$ results from water vapor from the southern coast to northern inland area by the southerly winds. The 7-days backward trajectory of air mass arriving at St. 9 supported this suggestion, showing that the majority of air mass was transported from northern Baffin Bay and eastern NOW.

We will add the description regarding the backward trajectory analysis as follows.

=====

2.3 Backward trajectory

To investigate the source region and transport pathway of water vapor and aerosols contained in ice core at the St. 9 site, we analysed air mass position along the backward trajectory from the St. 9 site during the past 7 days using the National Oceanographic and Atmospheric Administration (NOAA) Hybrid Single-Particle Lagrangian Integrated Trajectory (HYSPLIT) model (Stein et al., 2015) and National Centers for Environmental Prediction (NCEP) reanalysis data. The initial positions of air mass were set at 50, 500, 1000, 1500 m above ground level over the St. 9 site. The initial date and time were every 6 h from 2019 to 2023. We calculated the probability of the existence of an air mass with a 1° resolution. Considering the water vapor and aerosols supply from the ocean and

land surface, we excluded air mass over 1000 m above ground level. The existence probability was weighted by the daily amount of precipitation when the air mass arrived at the St. 9 site. The daily amount of precipitation was extracted from the ERA5 reanalysis dataset (Hersbach et al., 2020).

3.2.1 $\delta^{18}O$

The spatial variations in $\delta^{18}O$ in the surface snow showed maximum and minimum values at St. 3 (−19.12 ‰) and St. 9 (−37.21 ‰), respectively (Fig. S4a). The average $\delta^{18}O$ value from 0.00 to 1.01 m at St. 3 was greater than that at St. 9 (St. 3: −22.03 ‰; St. 9: −29.12 ‰) (Table 1). The $\delta^{18}O$ values in surface snow and the snowpack decreased from the seacoast toward the inland site. The past 7 days backward trajectory arriving at the St. 9 also exhibited that majority of air mass was transported from the south of the St. 9, situated on the northern Baffin Bay and eastern NOW (Fig. S5). We suggest that the south-to-north gradient of $\delta^{18}O$ results from water vapor, which originates from northern Baffin Bay and eastern NOW, transport from the southern coast to the northern inland area by southerly winds.

=====

Reviewer comment:

Line 216: Interpretation in Figure 6c should align with the seasonal framework in Figure 6b.

Author reply:

We will correct "summer to winter" to "spring-summer to autumn-winter" according to the seasonal framework of the dating in the snowpack at St. 9.

We will revise the text that you have pointed out as below.

=====

The difference in $\delta^{18}O$ values between St. 3 and St. 9 increased from spring–summer to autumn–winter from 2022–2023 and decreased until spring in 2023 (Fig. 3c).

=====

Reviewer comment:

Lines 222, 232: Revise for clarity.

Author reply:

We will revise the text that you have pointed out as below.

=====

Therefore, the difference of the Cl^-/Na^+ ratio in snowpack from sea-water ratio often reveals sea salt modification within the atmosphere.

=====

Reviewer comment:

Line 239: Provide supporting data

Author reply:

We will add the 7-days backward trajectory analysis (Fig. 1 in this file). We suggested the sea salt observed in this study could be transported along a short distance pathway without reactions with H_2SO_4 and HNO_3 during transportation. The backward trajectory analysis supported this suggestion, showing that the air mass frequency passed over the eastern NOW ocean, located near the St. 9, was high throughout the year.

Reviewer comment:

Line 278: Explain nitrate concentration increases due to melting/refreezing. if possible, explain shortly or provide references. Revise "positive peaks" to just "peaks."

Author reply:

The NO_3^- tend to move easily with meltwater and become concentrated during refreezing (Matoba et al., 2002). We will add this text to our manuscript.

We will correct the "positive peaks" to "peaks" in our revised manuscript.

Reviewer comment:

Table 1: Replace nss-K^+ with K^+ and nss-Mg^{2+} with Mg^{2+} data.

Author reply:

In accordance with your comment, we have replaced nssK^+ with K^+ and nssMg^{2+} with Mg^{2+} in Table 1 (in this file).

Table 1 (in this file). Mean values and standard deviations of several ion species and water stable isotopes between St. 3 and St. 9. The mean values at St.9 were obtained at depths from 0.00 to 1.01 m.

	Na^+ (μeq L^{-1})	NH_4^+ (μeq L^{-1})	K^+ (μeq L^{-1})	Mg^{2+} (μeq L^{-1})	nssCa^{2+} (μeq L^{-1})	MSA (μeq L^{-1})	Cl^- (μeq L^{-1})	nssSO_4^{2-} (μeq L^{-1})	NO_3^- (μeq L^{-1})	Cl^-/Na^+ (μeq L^{-1})	$\delta^{18}O$ (‰)	δD (‰)	d-excess (‰)
mean(St.3)	133.70	0.61	2.77	22.69	-0.46	0.01	155.53	1.51	1.32	1.19	-22.03	-160.27	15.93
std. (St.3)	181.51	0.45	4.26	27.51	0.87	0.02	206.34	3.45	1.19	0.15	2.22	17.58	2.12
mean(St.9)	34.17	0.04	0.68	7.11	0.85	0.01	41.37	0.40	0.60	1.17	-29.12	-218.69	14.29
std. (St.9)	54.12	0.22	1.25	9.12	3.67	0.01	65.33	0.92	0.44	0.12	6.46	52.27	2.66

Reviewer comment:

Avoid repeating earlier content. Summarize only the most significant findings and implications.

Author reply:

We will summarize the conclusion section as follows, and we will avoid some repetitions such as "western side of Prudhoe Land".

=====

4 Conclusion

We conducted glaciological observations from 9−11 April 2023 on the western side of Prudhoe Land in northwestern Greenland facing the NOW to elucidate the source conditions and transportation processes of water vapor and aerosols in this region. The dating of the snowpack at St. 9, which is located at the inland of the western side of Prudhoe Land, revealed that the layer at a depth of 4.20 m corresponded to 3.5 years. The average annual accumulation at St. 9 was 0.49 m w.eq. yr^{-1}.

The snowpacks on the western side of Prudhoe Land contained aerosols from distant sources, such as remote dust and anthropogenic aerosols, in early spring–summer layers. On the other hand, they also contained aerosols from local sources such as ocean biological activity and frost flowers in the NOW and local dust around the coast of northwestern Greenland during other seasons, unlike the inland of the Greenland Ice Sheet. Moreover, we noted that the snowpacks were able to trace the poleward heat and moisture transport event along Baffin Bay during winter.

Arctic climate warming caused decreases in the sea ice thickness and concentration over the last few decades in the NOW and could influence clouds and precipitation following changes in sea ice and biological activities in the NOW. We found for the first time that the environmental changes in the NOW can be elucidated by the snowpack and ice core on the western side of the Prudhoe Land. We suggest that the chemical substances in the deeper ice core from this region could help explain the multidecadal variations in the sea ice, biological activities, and related water and aerosol circulation around the NOW and could develop to understand the accurate future projections of environmental change in this region.

=====

References:

Kurosaki, Y., Matoba, S., Iizuka, Y., Niwano, M., Tanikawa, T., Ando, T., Hori, A., Miyamoto, A., Fujita, S., and Aoki, T.: Reconstruction of Sea Ice Concentration in Northern Baffin Bay Using Deuterium Excess in a Coastal Ice Core From the Northwestern Greenland Ice Sheet, JGR Atmospheres, 125, e2019JD031668, https://doi.org/10.1029/2019JD031668, 2020.

Matoba, S., Narita, H., Motoyama, H., Kamiyama, K., and Watanabe, O.: Ice core chemistry of Vestfonna Ice Cap in Svalbard, Norway, J. - Geophys. - Res., 107, https://doi.org/10.1029/2002JD002205, 2002b.

Matoba, S., Yamasaki, T., Miyahara, M., and Motoyama, H.: Spatial variations of δ18O and ion species in the snowpack of the northwestern Greenland ice sheet, Bulletin of Glacier Research, 32, 79–84, https://doi.org/10.5331/bgr.32.79, 2014.